ELECTRONIC SUPPORTING INFORMATION

Slow Relaxation of Magnetization in a $\{Fe_6Dy\}$ Complex Deriving from a Family of Highly Symmetric Metallacryptands

Angeliki A. Athanasopoulou[1,2], Luca M. Carrella [1] and Eva Rentschler [1,*]

1 Institute of Inorganic and Analytical Chemistry, Johannes Gutenberg University Mainz, Duesbergweg 10-14, D-55128 Mainz, Germany

2 Graduate School Materials Science in Mainz, Staudinger Weg 9, D-55128 Mainz, Germany

*Corresponding author

Eva Rentschler

Institute of Inorganic and Analytical Chemistry

Johannes Gutenberg University Mainz

Duesbergweg 10-14

D-55128 Mainz, Germany

Fax: +49 6131 39 23922

Tel: +49 6131 39 25491

E-mail: rentschler@uni-mainz.de

Experimental Section

All manipulations were performed under aerobic conditions using materials (reagent grade) and solvents as received.

C, H and N elemental analyses were carried out on a Foss Heraeus Vario EL at the Institute of Organic Chemistry at the Johannes Gutenberg University Mainz. Infrared absorption spectra were recorded at room temperature in a range of 3,000-400 cm^{-1} on a Thermo Fischer NICOLET Nexus FT/IR-5700 spectrometer equipped with Smart Orbit ATR Diamond cell. UV-Vis absorption measurements were performed between for complexes 1, 2, 3 and 4 in MeCN between 200 and 1000 nm on a JASCO V-570 UV/Vis/NIR spectrophotometer (Fig.S10, ESI) Variable-temperature direct current (dc) magnetic susceptibility measurements were performed on polycrystalline samples with the use of Quantum Design SQUID magnetometer MPMS-7 equipped with a 7 T magnet. The samples were embedded in eicosane to avoid orientation of the crystallites under applied field. Experimental susceptibility data were corrected for the underlying diamagnetism using Pascal's constants.[1] The temperature dependent magnetic contribution of the holder and of the embedding matrix eicosane were experimentally determined and substracted from the measured susceptibility data. Variable temperature susceptibility data were collected in a temperature range of 2-300K under an applied field of 0.1 Tesla, while magnetization data were collected between 2 and 10 K and using magnetic fields up to 7 Tesla. Alternating-current (ac) measurements were performed with an oscillating magnetic field of 3 Oe at frequencies ranging from 1 to 1400 Hz. Field-dependence measurements were performed and they revealed an optimum dc field of 800 Oe. Using that optimum field further magnetic measurements were performed as described in the text.

Synthesis of reported compounds 1-4:

$(pipH)_3\{Fe_6Gd(shiH)_3(shi)_6\}\cdot 1.5\ pip\cdot xH_2O$ (1): To a stirred almost colorless solution of $shiH_3$ (30.50 mg, 0.2 mmol) and piperidine (20 µL, 0.2 mmol) in MeOH, $Fe(acac)_3$ (0.071 mg, 0.2 mmol) was added and left for stirring for 5 min. To the resulting dark red almost clear solution $Gd(NO_3)_3{\cdot}H_2O$ (7.00 mg, 0.025 mmol) was added along with $^tBu_4NClO_4$ (26.00 mg, 0.075 mmol) and was stirred for further 40 min. Then, the solution was filtered and the filtrate was layered with Et_2O/hexane. Slow mixing gave diffraction quality crystals of **1** after 5 days which were collected by filtration, washed with hexanes (3 × 5 mL) and dried in air. Yield: 0.045 g (72.5%) based on the Gd^{III} ion. The air-dried solid was analyzed as **$1\cdot 1.5pip\cdot 15H_2O$ ($Fe_6Gd_1H_{121.5}O_{42}C_{85.5}N_{13.5}$):** C, 40.99; H, 4.89; N, 7.55. Found: C, 41.05; H, 4.81; N, 7.54. Selected ATR data (cm^{-1}): 1593 (w), 1560 (w), 1485 (s), 1429 (w), 1305 (w), 1254 (s), 1035 (w), 916 (s), 848 (w), 664 (w), 582 (s), 541 (w).

$(pipH)_3\{Fe_6Dy(shiH)_3(shi)_6\}\cdot 1.5\ pip\cdot xH_2O$ (2): This complex was prepared in the same manner as complex **1** but using $Dy(NO_3)_3{\cdot}H_2O$ (9.00 mg, 0.025 mmol) instead of $Gd(NO_3)_3{\cdot}H_2O$. After 7 days dark brown crystals of **2** appeared; these were collected by filtration, washed with hexanes (3 × 5 mL) and dried in air. Yield: 0.042 g (68%) based on the Dy^{III} ion. The air-dried solid was analyzed as **2·1.5pip·11H$_2$O (Fe$_6$Dy$_1$H$_{113.5}$O$_{38}$C$_{85.5}$N$_{13.5}$):** C, 42.20; H, 4.70; N, 7.77. Found: C, 42.28; H, 4.62; N, 7.74. Selected ATR data (cm^{-1}): 1591 (w), 1560 (w), 1485 (s), 1431 (w), 1305 (w), 1253 (s), 1035 (w), 917 (s), 849 (w), 666 (w), 581 (s), 541 (w).

(pipH)$_3${Fe$_6$Tb(shiH)$_3$(shi)$_6$}·1.5 pip·xH$_2$O (3): The complex was prepared in the same manner as the complexes above but using Tb(NO$_3$)$_3$·H$_2$O (9.00 mg, 0.025 mmol) as the lanthanide source . After 5 days dark brown crystals of **3**; these were collected by filtration, washed with hexanes (3 × 5 mL) and dried in air. Yield: 0.039 g (63%) based on the Tb^{III} ion. The vacuum-dried solid was analyzed as **3·1.5pip·14H$_2$O (Fe$_6$Tb$_1$H$_{119.5}$O$_{41}$C$_{85.5}$N$_{13.5}$):** C, 41.29; H, 4.84; N, 7.60. Found: C, 41.28; H, 4.75; N, 7.49. Selected ATR data (cm^{-1}): 1592 (w), 1560 (w), 1485 (s), 1428 (w), 1305 (w), 1255 (s), 1036 (w), 916 (s), 848 (w), 665 (w), 582 (s), 542 (w).

(pipH)$_3${Fe$_6$Y(shiH)$_3$(shi)$_6$}·1.5 pip·xH$_2$O (4): The complex was prepared in the same manner as the complexes above but with the use of Y(NO$_3$)$_3$·H$_2$O (10.00 mg, 0.025 mmol) as the lanthanide source. After 8 days dark brown crystals of **4**; these were collected by filtration, washed with hexanes (3 × 5 mL) and dried in air. Yield: 0.039 g (52%) based on the Y^{III} ion. The vacuum-dried solid was analyzed as **4·1.5pip·11H$_2$O (Fe$_6$Y$_1$H$_{113.5}$O$_{38}$C$_{85.5}$N$_{13.5}$):** C, 43.09; H, 4.88; N, 7.92. Found: C, 43.19; H, 4.82; N, 7.81. Selected ATR data (cm^{-1}): 1592 (w), 1560 (w), 1485 (s), 1428 (w), 1305 (w), 1255 (s), 1036 (w), 916 (s), 848 (w), 665 (w), 582 (s), 542 (w).

Single-crystal X-ray diffraction studies.

X-ray diffraction data for the structure analysis were collected from suitable single crystals on a STOE IPDS 2T [2–5] equipped with an Oxford cooling system operating at 120(2)K (**1**) and at 193(**2**) K [3–5], respectively. Graphite-monochromated Mo-Kα radiation (λ = 0.71073 Å) from long-fine focus sealed X-ray tube was used throughout. Data indexing, reduction, integration and absorption correction were done with STOE X-AREA and STOE X-RED[2]. Structures were solved with SHELXT[3] and refined by full-matrix least-squares on F-squared using SHELXL[4], interfaced through OLEX2[5]. All non-hydrogen atoms were refined with anisotropic displacement parameters, while hydrogen atoms belonging to the main core have been placed on idealized position using a riding model. The hydrogen atoms of the doubly deprotonated ligands were placed according to charge balance considerations and geometrical reasons. For the solvent water molecules the hydrogen atoms were placed geometrical. For the solvent water molecules the hydrogen atoms cannot be located satisfactorily and were omitted. Although some water molecules can be located, still large solvent accessible voids are present in the structures. The highly disordered solvent molecules in these voids were squeezed with the routine SQUEEZE[6–8] implemented in Platon[7]. The piperidinium cation is disordered over two positions with a site occupation of 0.6/0.4. CCDC 1873575-1873578 contains the supplementary crystallographic data for the structure reported in this paper. These data can be obtained free of charge via www.ccdc.cam.ac.uk/conts/retrieving.html (or from the Cambridge Crystallographic Data Centre, 12 Union Road, Cambridge CB21EZ, UK; fax: (+44)1223-336-033; or deposit@ccdc.cam.ac.uk).

Table S1 Crystallographic data for complexes **1-4.**

Complex	**1**	**2**	**3**	**4**
Empirical formula	$C_{85.5}H_{91.50}Fe_6GdN_{13.5}O_{45}$	$C_{85.5}H_{93}DyFe_6N_{13.5}O_{43.5}$	$C_{85.5}H_{91.5}TbFe_6N_{13.5}O_{45}$	$C_{85.5}H_{91.5}YFe_6N_{13.5}O_{46.25}$
Formula weight	2520.59	2503.35	2522.26	2472.25
Temperature/K	120(2)	193(2)	193(2)	193(2)
Crystal system	trigonal	trigonal	trigonal	trigonal
Space group	P $\bar{3}$c 1	P $\bar{3}$c 1	P $\bar{3}$c 1	P $\bar{3}$c 1
a/Å	20.306(2)	20.474(3)	20.715(3)	20.6406(5)
b/Å	20.306(2)	20.474(3)	20.715(3)	20.6406(5)
c/Å	36.6668(4)	36.848(7)	37.100(7)	37.0102(11)
α/°	90	90	90	90
β/°	90	90	90	90
γ/°	120	120	120	120
Volume/Å^3	13094(3)	13377(5)	13787(5)	13655.2(8)
Z	3.99996	3.99996	3.99996	3.99996
ρ_{calc}g/cm^3	1.279	1.243	1.215	1.203
μ/mm^{-1}	1.222	1.258	1.193	1.115
F(000)	5116.0	5082	5120	5056.0
Crystal size/mm^3	0.23 × 0.157 × 0.12	0.18 × 0.16 × 0.13	0.42 × 0.393 × 0.34	0.26 × 0.137 × 0.06
Radiation	MoK\α (λ = 0.71073)	MoK\α (λ = 0.71073)	MoK\α (λ = 0.71073)	MoK\α (λ = 0.71073)
2Θ range for data collection/°	4.162 to 57.018	4.13 to 56.976	4.082 to 56.952	4.958 to 51.99
Index ranges	-21 ≤ h ≤ 27 -27 ≤ k ≤ 27 -46 ≤ l ≤ 48	-26 ≤ h ≤ 25 -24 ≤ k ≤ 27 -48 ≤ l ≤ 49	-27 ≤ h ≤ 26 -27 ≤ k ≤ 27 -49 ≤ l ≤ 48	-22 ≤ h ≤ 25 -25 ≤ k ≤ 22 -45 ≤ l ≤ 45
Reflections collected	48829	44898	68203	50806
Independent reflections	R_{int} = 0.0256 R_{sigma} = 0.0191	R_{int} = 0.0417 R_{sigma} = 0.0394	R_{int} = 0.0570 R_{sigma} = 0.0268	R_{int} = 0.1053 R_{sigma} = 0.0539
Data/restraints/ parameters	10867 / 114 / 562	11114/ 303/ 544	11553/ 120/ 553	8957/ 160/ 556
Goodness-of-fit on F^2	1.077	1.111	1.143	1.121
Final R^{a,b} indexes [I>=2σ (I)]	R_1 = 0.0533 wR_2 = 0.1436	R_1 = 0.0744 wR_2 = 0.1872	R_1 = 0.0572 wR_2 = 0.1699	R_1 = 0.0846 wR_2 = 0.2312
Final R^{a,b} indexes [all data]	R_1 = 0.0645 wR_2 = 0.1513	R_1 = 0.1169 wR_2 = 0.2189	R_1 = 0.0762 wR_2 = 0.1856	R_1 = 0.1292 wR_2 = 0.2695
Largest diff. peak /hole / e Å^{-3}	1.03 / -1.28	1.08/ -1.84	0.751/ -0.374	0.88/ -0.59

$^aR_1 = \Sigma(||F_o| - |F_c||)/\Sigma|F_o|$. $^bwR_2 = [\Sigma[w(F_o^2 - F_c^2)^2]/\Sigma[w(F_o^2)^2]]^{1/2}$, $w = 1/[\sigma^2(F_o^2) + (ap)^2 + bp]$, where $p = [\max(F_o^2, 0) + 2F_c^2]/3$.

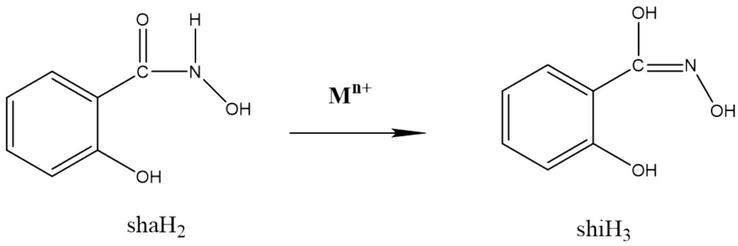

Scheme 1. Illustrative representation and abbreviation of organic molecules discussed in the text.

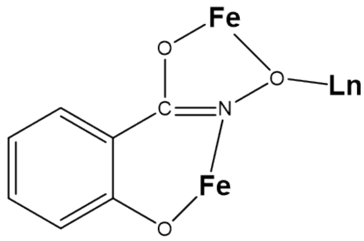

$\eta^1:\eta^1:\eta^1:\eta^2:\mu_3$

Figure S1: Coordination mode of shi^{3-} in complexes **1**-**4**.

Table S2 Selected Bond Lengths for complexes **1-4.**

Atom	Atom	Length/Å
Dy1	O2	2.373(4)
Dy1	O5	2.362(4)
Dy1	O8	2.549(4)
Fe1	O1^{2}	1.998(4)
Fe1	O2^{2}	2.038(4)
Fe1	O3	1.972(5)
Fe1	O9	1.991(5)
Fe1	N1	2.113(6)
Fe1	N3	2.065(5)
Fe2	O4^{2}	2.033(5)
Fe2	O5^{2}	2.015(4)
Fe2	O6	1.985(5)
Fe2	O7	1.951(5)
Fe2	O8	2.094(4)
Fe2	N2	2.027(6)
O2	N1	1.419(6)
O5	N2	1.407(6)
O8	N3	1.419(7)
Gd1	O2	2.384(3)
Gd1	O5	2.397(3)
Gd1	O8	2.548(3)
Fe1	O1^{1}	2.036(3)
Fe1	O2^{1}	2.012(3)
Fe1	O3	1.982(3)
Fe1	O8	2.097(2)
Fe1	O9	1.953(3)
Fe1	N1	2.031(3)
Fe2	O4^{1}	2.007(3)
Fe2	O5^{1}	2.028(3)
Fe2	O6	1.980(3)
Fe2	O7	1.988(3)
Fe2	N2	2.122(3)
Fe2	N3	2.071(3)
O2	N1	1.396(5)
O5	N2	1.412(4)
O8	N3	1.416(5)
Tb1	O2	2.387(3)
Tb1	O5	2.382(3)
Tb1	O8	2.558(3)
Fe1	O1^{2}	2.002(3)
Fe1	O2^{2}	2.034(3)
Fe1	O3	1.979(3)

Fe1	O9	1.992(3)
Fe1	N1	2.128(4)
Fe1	N3	2.064(4)
Fe2	O4[2]	2.034(3)
Fe2	O5[2]	2.012(3)
Fe2	O6	1.985(3)
Fe2	O7	1.954(4)
Fe2	O8	2.092(3)
Fe2	N2	2.028(4)
O2	N1	1.416(5)
O5	N2	1.401(5)
O8	N3	1.410(5)
Y1	O2	2.361(4)
Y1	O5	2.372(4)
Y1	O8	2.546(5)
Fe1	O1[1]	2.031(5)
Fe1	O2[1]	2.018(5)
Fe1	O3	1.992(5)
Fe1	O7	1.955(5)
Fe1	O8	2.095(4)
Fe1	N1	2.024(6)
Fe2	O4[1]	2.001(5)
Fe2	O5[1]	2.035(5)
Fe2	O6	1.973(5)
Fe2	O9	1.991(5)
Fe2	N2	2.118(6)
Fe2	N3	2.059(5)
O2	N1	1.395(7)
O5	N2	1.418(7)
O8	N3	1.415(7)

[1]1+Y-X,1-X,+Z; [2]1-Y,+X-Y,+Z; [3]-Y+X,-Y,3/2-Z

Table S3 Selected Bond Angles for **1-4.**

	Atom	Atom	Angle/°
$O2^{1}$	Dy1	O2	76.99(15)
O2	Dy1	O8	70.73(14)
$O2^{1}$	Dy1	O8	77.55(14)
$O2^{2}$	Dy1	$O8^{2}$	70.73(14)
O2	Dy1	$O8^{1}$	142.47(15)
O5	Dy1	$O2^{2}$	130.47(13)
O5	Dy1	O2	88.33(15)
O5	Dy1	$O8^{2}$	59.91(14)
O5	Dy1	O8	67.88(14)
O5	Dy1	$O8^{1}$	129.20(14)
$O8^{1}$	Dy1	O8	118.61(4)
$O1^{1}$	Fe1	$O2^{1}$	77.13(17)
$O1^{1}$	Fe1	N1	96.7 (2)
$O1^{1}$	Fe1	N3	159.3(2)
$O2^{1}$	Fe1	N1	83.6(2)
N3	O8	Dy1	115.6(3)
O2	N1	Fe1	122.5(4)
O2	N2	Fe2	116.5(4)
O2	Gd1	$O2^{1}$	77.55(11)
O2	Gd1	$O5^{1}$	145.28(10)
O2	Gd1	O5	88.21(10)
$O2^{1}$	Gd1	O5	130.37(10)
O2	Gd1	O8	67.69(10)
O2	Gd1	$O8^{1}$	128.99(10)
$O2^{1}$	Gd1	O8	59.72(10)
O5	Gd1	$O5^{1}$	77.12(10)
O5	Gd1	O8	70.84(10)
O5	Gd1	$O8^{1}$	142.80(9)
O5	Gd1	$O8^{2}$	77.75(10)
O8	Gd1	$O8^{1}$	118.51(3)
$O1^{1}$	Fe1	O8	149.15(13)
$O2^{1}$	Fe1	$O1^{1}$	76.50(12)
$O2^{1}$	Fe1	O8	73.53(10)
$O2^{1}$	Fe1	N1	90.44(14)
N3	O8	Gd	115.0(2)
N3	O8	Fe1	109.8(2)
O2	N1	Fe1	117.0(3)
O5	N2	Fe2	122.7(2)
$O2^{1}$	Tb1	$O2^{2}$	77.03(11)
$O2^{1}$	Tb1	O8	77.40(10)

O2	Tb1	O8[1]	142.86(10)
O2	Tb1	O8	71.30(10)
O5	Tb1	O2	88.23(11)
O5[1]	Tb1	O2	130.95(11)
O5	Tb1	O2[1]	144.74(11)
O5[1]	Tb1	O5	77.49(11)
O5	Tb1	O8	67.52(10)
O5	Tb1	O8[2]	59.82(10)
O8[1]	Tb1	O8	118.49(3)
O1[1]	Fe1	O2[1]	76.97(13)
O1[1]	Fe1	N1	96.96(15)
O1[1]	Fe1	N3	159.10(15)
O2[1]	Fe1	N1	83.59(14)
N3	O8	Tb1	115.5(2)
N3	O8	Fe2	110.4(2)
O2	N1	Fe1	122.5(3)
O5	N2	Fe2	116.8(3)
O2	Y1	O2[1]	77.44(17)
O2	Y1	O5[1]	144.87(16)
O2	Y1	O5	88.29 (16)
O2	Y1	O5[2]	130.87(16)
O2	Y1	O8[1]	129.05(15)
O2	Y1	O8[2]	59.88(15)
O2	Y1	O8	67.74(15)
O5	Y1	O5[2]	77.00(17)
O5	Y1	O8[2]	77.30(15)
O5	Y1	O8[1]	142.66(15)
O5	Y1	O8	71.15(15)
O8	Y1	O8[1]	118.56(4)
O1[1]	Fe1	O8	148.7(2)
O2[1]	Fe1	O1[1]	76.76(18)
O2[1]	Fe1	O8	73.23(17)
O2[1]	Fe1	N1	89.6(2)
N3	O8	Y1	115.7(3)
N3	O8	Fe1	110.1(4)
O2	N1	Fe1	117.0(4)
O5	N2	Fe2	122.9(4)

[1]1-Y,+X-Y,+Z; [2]1+Y-X,1-X,+Z; [3]-Y+X,-Y,3/2-Z

Table S4: Bond Valence Sum Calculations (BVS) for complexes **1**-**4**.

Atom	Complex **1**		Complex **2**		Complex **3**		Complex **4**	
	+2	**+3**	**+2**	**+3**	**+2**	**+3**	**+2**	**+3**
Fe1	2.65	**3.13**	2.63	**3.08**	2.60	**3.05**	2.63	**3.11**
Fe2	2.61	**3.06**	2.65	**3.13**	2.65	**3.13**	2.62	**3.07**

Table S5. Shape measurements of the 9-coordinate lanthanide coordination polyhedra. The bold numbers indicate the closest polyhedron according to SHAPE calculations.[9]

Polyhedron[c]	Gd1	Dy1	Tb1	Y1
EP-9	35.38	35.34	35.44	35.35
OPY-9	23.56	23.52	23.50	23.52
HBPY-9	19.89	19.95	20.09	20.03
JTC-9	12.76	12.73	12.76	12.81
JCCU-9	10.51	10.47	10.58	10.53
CCU-9	9.53	9.56	9.64	9.60
JCSAPR-9	2.54	2.49	2.49	2.48
CSAPR-9	1.76	1.77	1.74	1.75
JTCTPR-9	1.89	1.78	1.81	1.78
TCTPR-9	**1.13**	**1.14**	**1.11**	**1.12**
JTDIC-9	10.64	10.66	10.76	10.80
HH-9	12.63	12.65	12.65	12.66
MFF-9	2.02	2.05	2.01	2.02

[c] Abbreviations: EP-9, enneagon; OPY-9, octagonal pyramid; HBPY-9, heptagonal bipyramid; JTC-9, Johnson triangular cupola J3; JCCU-9,capped cube J8; CCU-9, spherical-relaxed capped cube; JCSAPR-9, capped square antiprism J10; CSAPR-9, spherical capped square antiprism; JTCTPR-9, tricapped trigonal prism J51; TCTPR-9, spherical tricapped trigonal prism; JTDIC-9,tridiminished icosahedron J63; HH-9, hula-hoop; MFF-9, muffin.

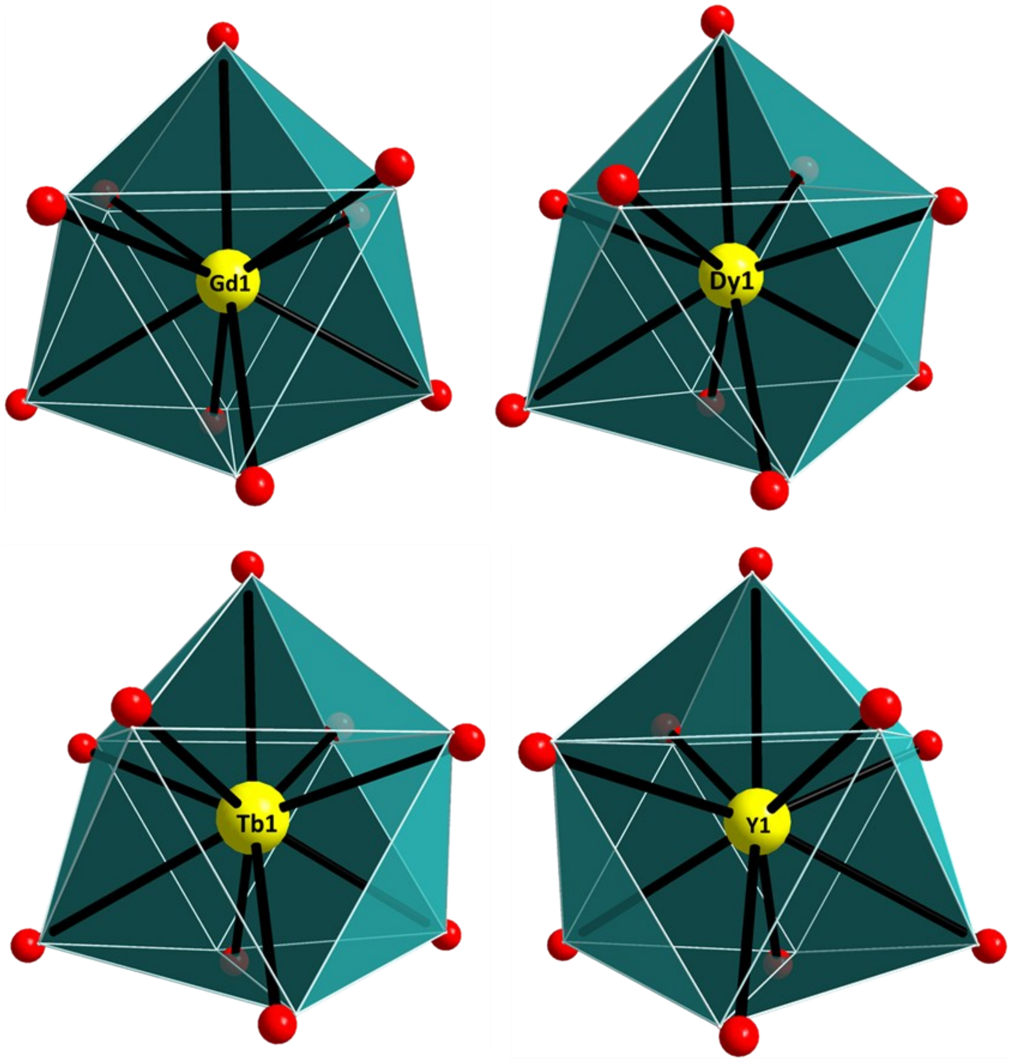

Figure S2: Spherical tricapped trigonal prismatic geometry of central lanthanide in complexes **1**-**4**. The points connected by the lighter lines define the vertices of the ideal polyhedron**.** Color scheme: Ln, yellow; O, red.

Table S6. Shape measurement of the 6 Fe(III) centers surrounding the lanthanide metal ion (in this case Dy) and respecting coordination polyhedra. The bold numbers indicate the closest polyhedron according to SHAPE calculations.

Polyhedron[c]	Fe_6
HP-6	34.32
PPY-6	17.55
OC-6	10.45
TPR-6	**0.88**
JPPY-6	21.71

[c] Abbreviations: HP-6, hexagon; PPY-6, pentagonal pyramid; OC-6, octahedron; TPR-6, trigonal prism; JPPY-6, Johnson pentagonal pyramid J2.

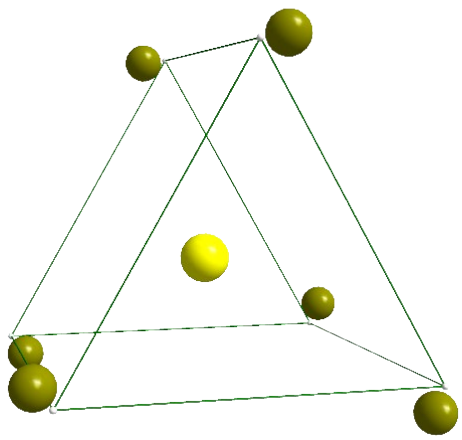

Figure S3: Trigonal prismatic geometry of Fe(III) ions in complex **2**. The points connected by the lighter lines define the vertices of the ideal polyhedron**.** Color scheme: Dy, yellow; Fe, dark yellow.

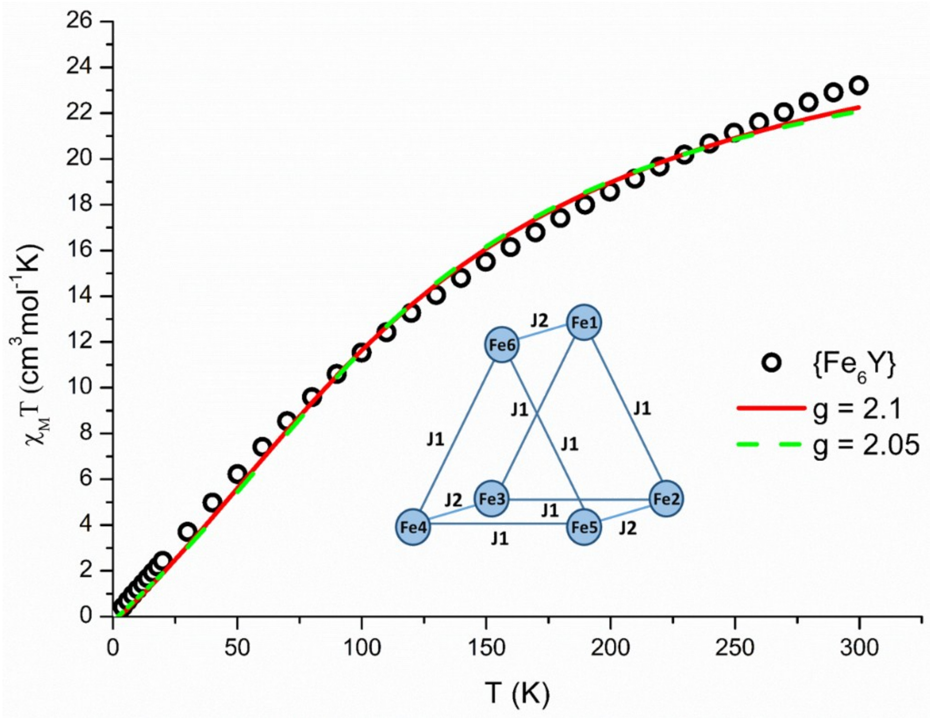

Figure S4: Temperature dependence of magnetic susceptibility for complex **4**. Red solid line and green dotted line represent fitting of the data in complex **4.** (Inset): fitting model for compound **4**.

Aiming to a better insight in the strength of the intramolecular Fe^{III} - Fe^{III} magnetic exchange interactions, the magnetic susceptibility data of complex **4** were fit using the CLUMAG[10] program. The magnetic susceptibility data of complex **4**, which comprises the diamagnetic Y^{III} ion in the central cavity, were fit using a 2-J model according to the spin Hamiltonian:

$$\hat{H} = -J_1 (\hat{S}_{Fe1}\cdot\hat{S}_{Fe2} + \hat{S}_{Fe2}\cdot\hat{S}_{Fe3} + \hat{S}_{Fe3}\cdot\hat{S}_{Fe1} + \hat{S}_{Fe4}\cdot\hat{S}_{Fe5} + \hat{S}_{Fe5}\cdot\hat{S}_{Fe6} + \hat{S}_{Fe4}\cdot\hat{S}_{Fe6}) - J_2(\hat{S}_{Fe1}\cdot\hat{S}_{Fe6} + \hat{S}_{Fe2}\cdot\hat{S}_{Fe5} + \hat{S}_{Fe3}\cdot\hat{S}_{Fe4})$$

Despite all our attempts for a better fitting of the data, the best fit parameters were obtained according to the depiction of the values on the graph above. The values that were obtained from the first attempt were J_1= +1.02 cm^{-1}, J_2 = - 9.60 cm^{-1} and g = 2.1, while the second best fitting attempt gave us J_1 = +1.86 cm^{-1}, J_2 = -9.40 cm^{-1} and g = 2.05. In both cases a TIP of 1.2*10-5 emu*mol^{-1} was employed. The g values in both cases are higher than expected for six-coordinate Fe(III) ions, with a d^5 electronic configuration, nevertheless no other fitting endeavors gave us more reliable results. A 1-J model was tested as well, considering the high symmetry of our molecule, with no success. Fitting attempts while employing more exchange coupling parameters were averted in order to avoid overparameterization, which in turn would not be reliable, based on the symmetric distances and angles of our compound.

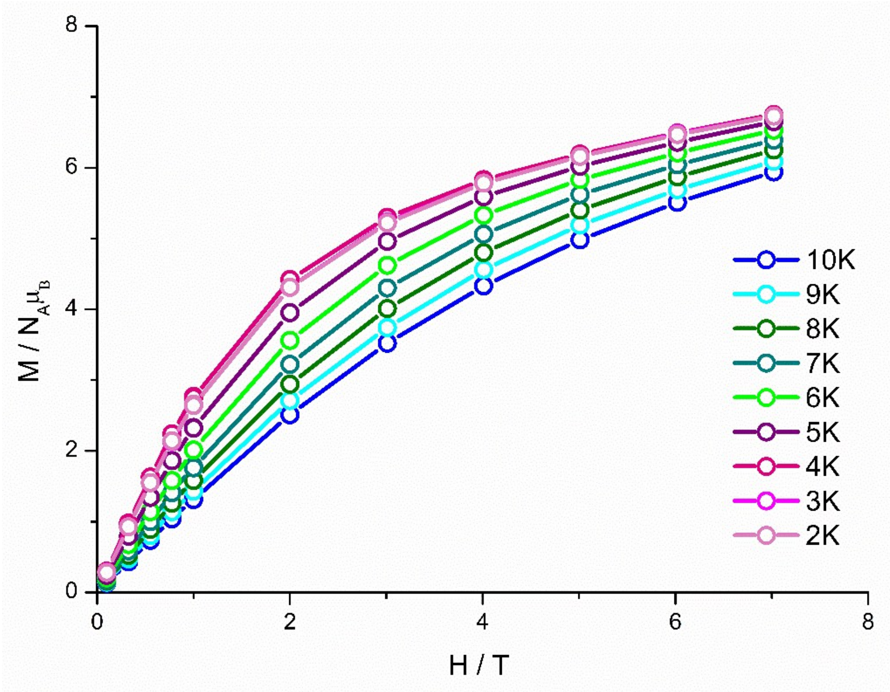

Figure S5: M vs H plots for complex **1** in various temperatures as indicated. Solid lines are guidelines for the eyes.

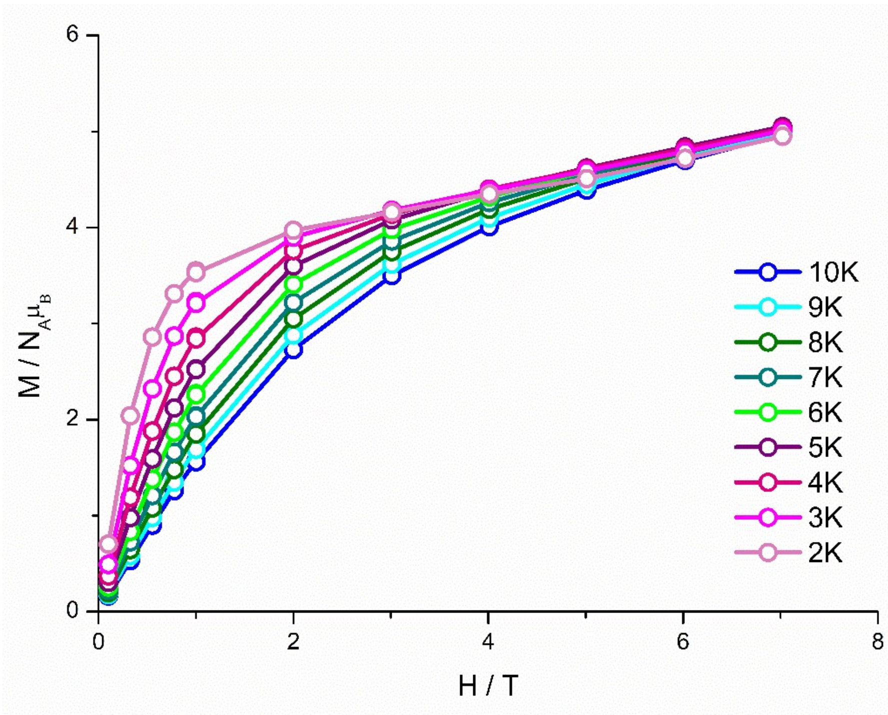

Figure S6: M vs H plots for complex **2** in various temperatures as indicated. Solid lines are guidelines for the eyes.

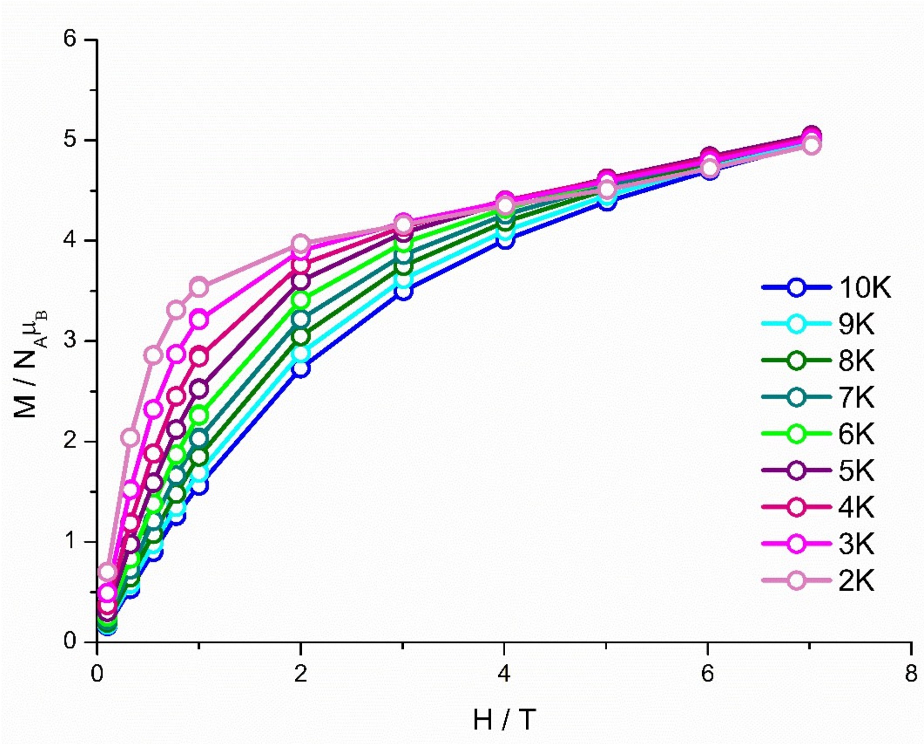

Figure S7: M vs H plots for complex **3** in various temperatures as indicated. Solid lines are guidelines for the eyes.

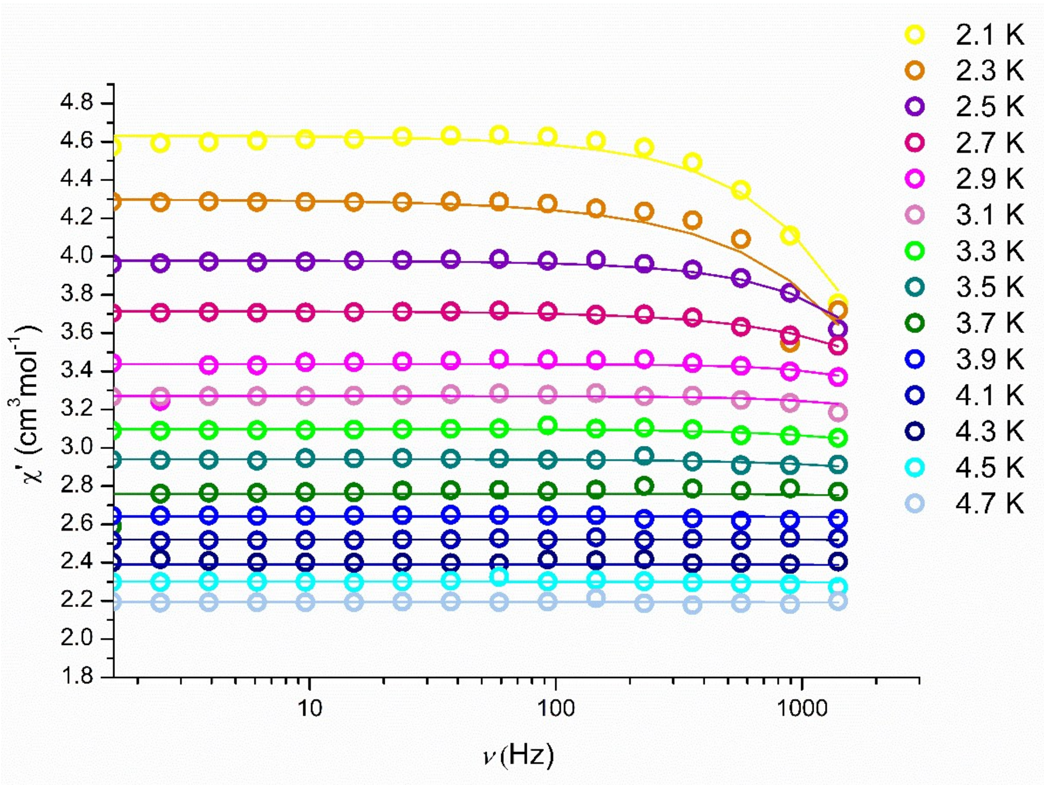

Figure S8: Frequency dependent in-phase susceptibility plot of for compound **2** (2.1 to 4.7 K) at zero field. Solid lines represent fit of the data.

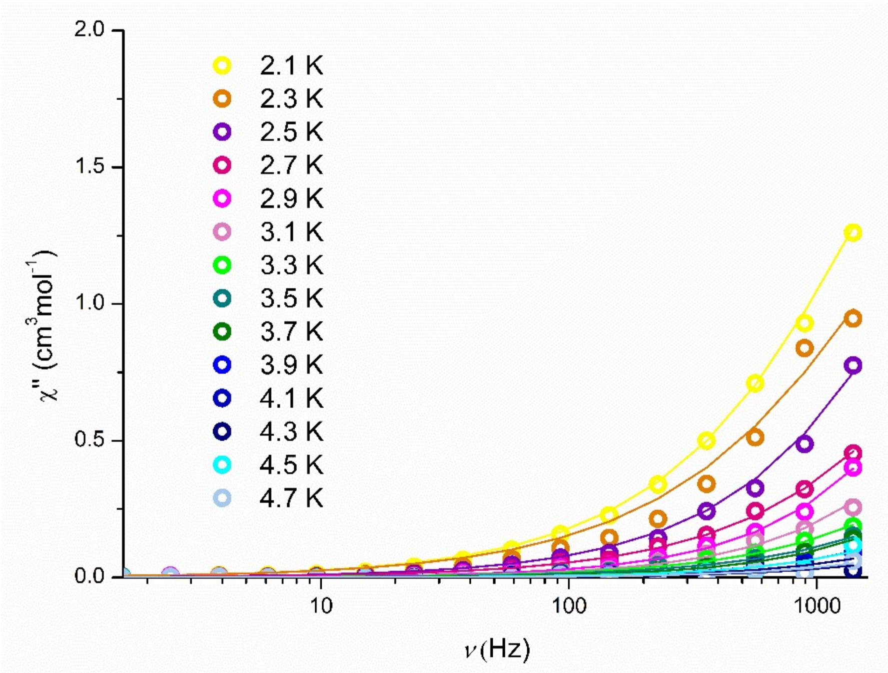

Figure S9: Frequency dependent out-of-phase susceptibility plot of for compound **2** (2.1 to 4.7 K) at zero field. Solid lines represent fit of the data.

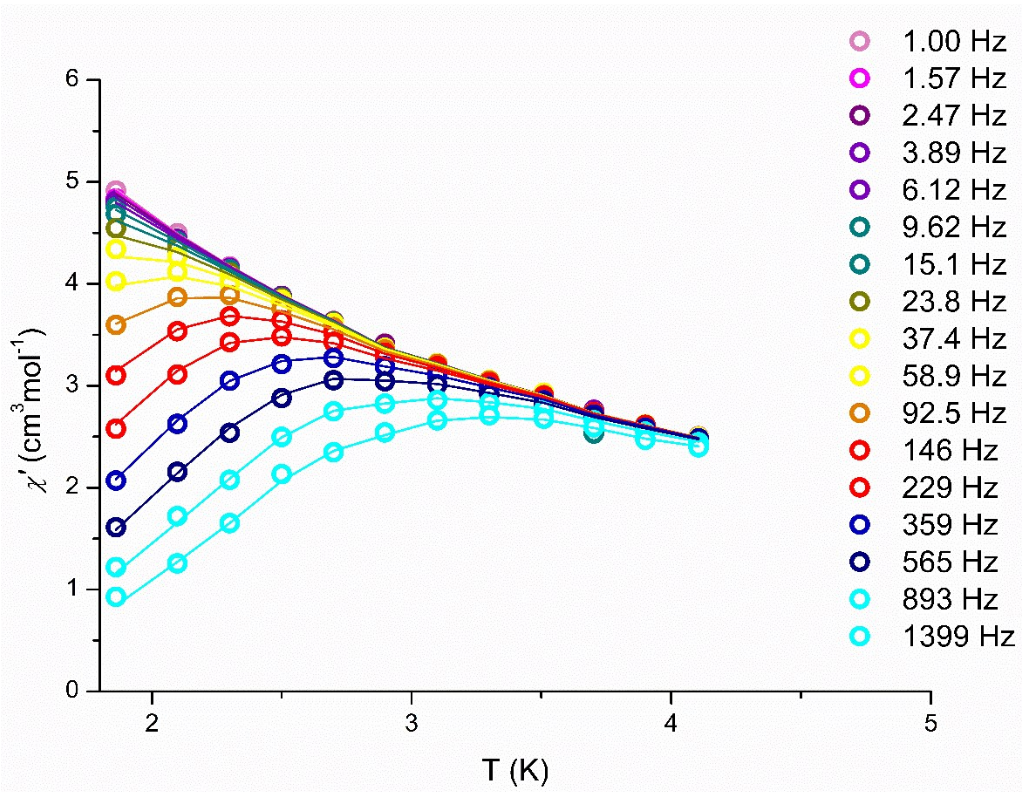

Figure S10: Temperature dependent in-phase susceptibility plot of for compound **2** (2.1 to 4.1 K) at 800 Oe. Solid lines represent fit of the data.

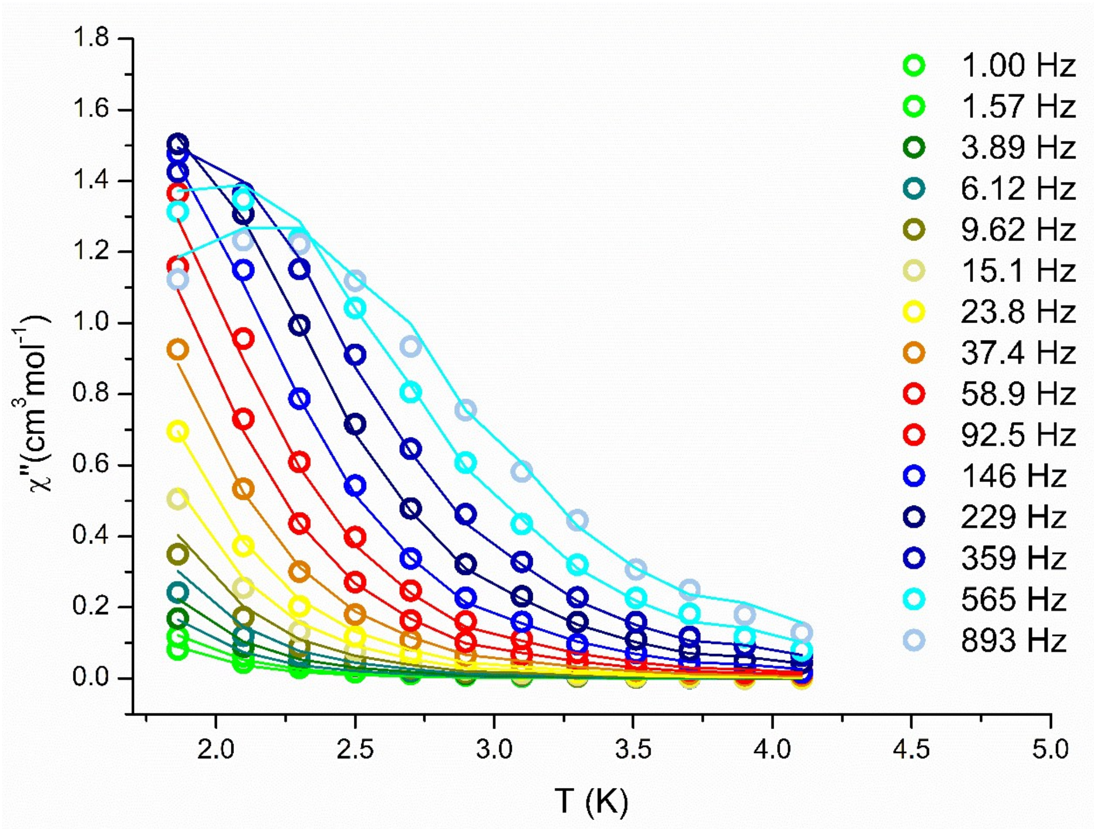

Figure S11: Temperature dependent out-of-phase susceptibility plot of for compound **2** (2.1 to 4.1 K) at 800 Oe. Solid lines represent fit of the data.

UV-Vis Absorption Spectroscopy

The ligand ($shiH_3$) has two main bands at 227 nm and 318 nm, which appear to be also present at all the complexes. These ligand-centered transitions, that can be assigned to excitations within the delocalized π-system of the coordinated hydroxamic acid, are observed at 210 and 307 nm for **1**, at 212 and 320 nm for **2**, at 219 and 312 nm for **3** and at 211 and 334 nm for **4**. The light absorption by **1** , **2**, **3** and **4** at around ~460 nm is characteristic for ligand-to-metal charge-transfer (LMCT) transitions.[11]

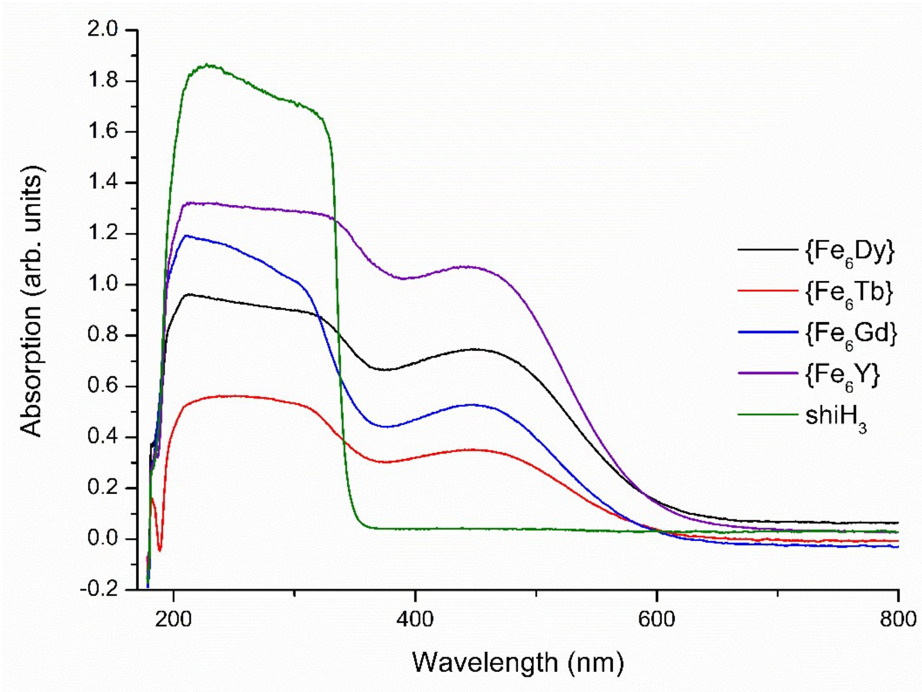

Figure S12: UV-Vis spectra of **1** (blue), **2** (black), **3** (red), **4** (purple) and shiH_3 (green) in MeCN.

Infrared Absorption Spectroscopy

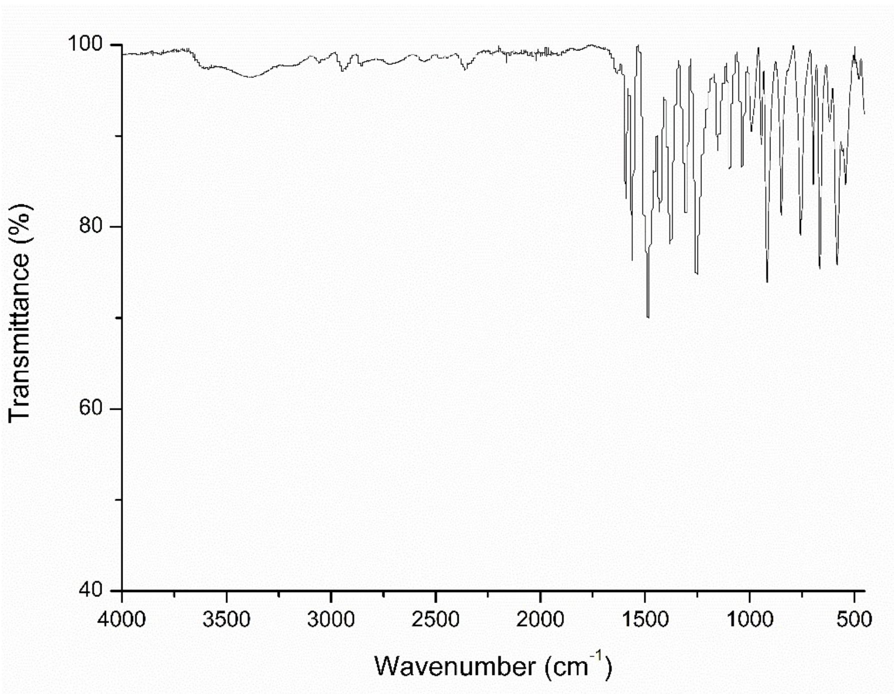

Figure S13: IR spectrum for complex **1**.

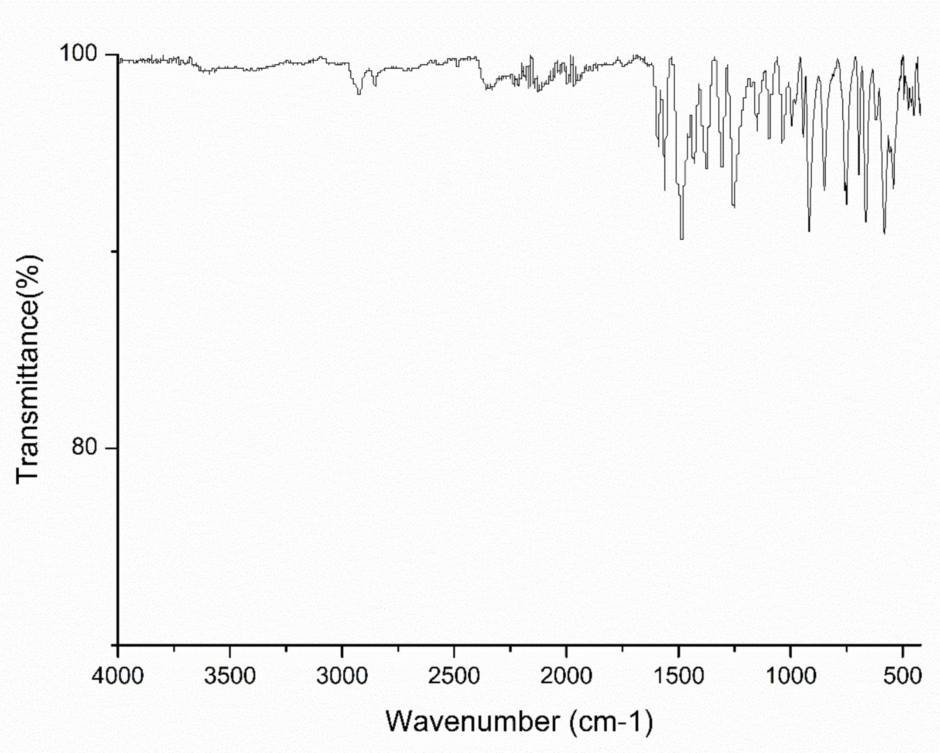

Figure S14: IR spectrum for complex **2**.

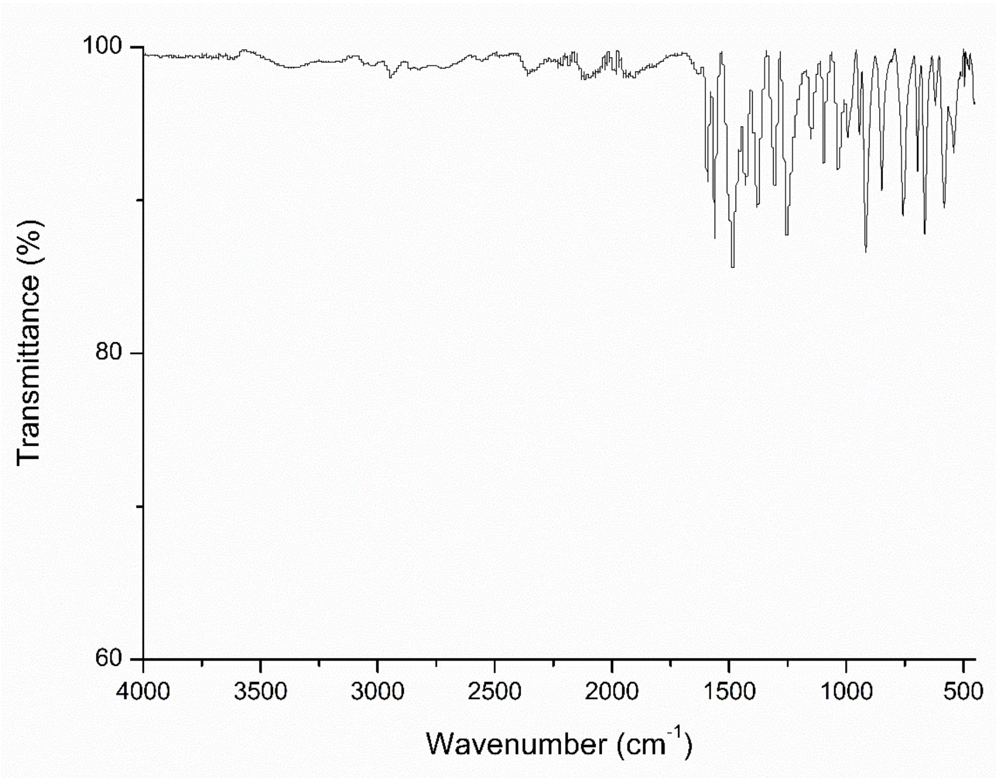

Figure S15: IR spectrum for complex **3**.

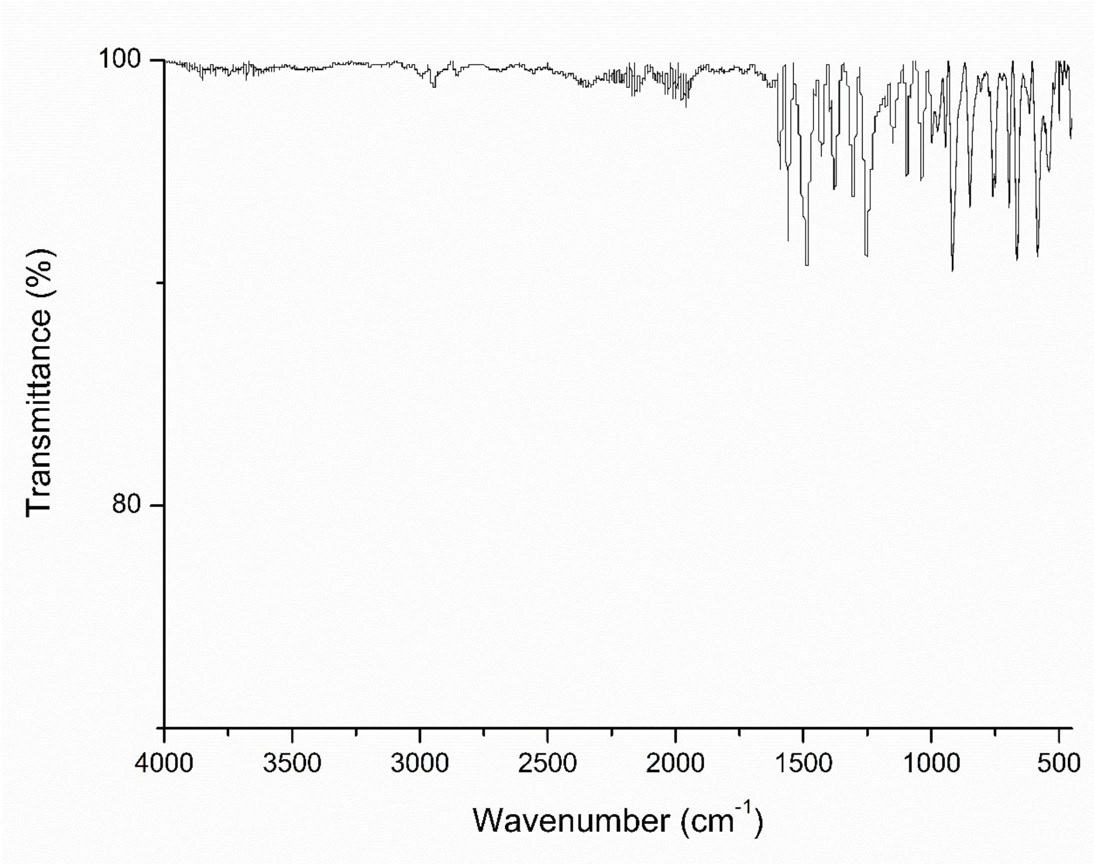

Figure S16: IR spectrum for complex **4**.

References

1 G. A. Bain and J. F. Berry, *Journal of Chemical Education*, 2008, **85**, 532.

2 Stoe & Cie X-AREA 2002, Stoe & Cie X-RED 2002, Stoe & Cie, Darmstadt, Germany.

3 G. M. Sheldrick, *Acta Crystallographica Section A Foundations and Advances*, 2015, **71**, 3–8.

4 G. M. Sheldrick, *Acta Crystallographica Section C Structural Chemistry*, 2015, **71**, 3–8.

5 O. V. Dolomanov, L. J. Bourhis, R. J. Gildea, J. A. K. Howard and H. Puschmann, *Journal of Applied Crystallography*, 2009, **42**, 339–341.

6 A. L. Spek, *Journal of Applied Crystallography*, 2003, **36**, 7–13.

7 A. L. Spek, *Acta Crystallographica Section D Biological Crystallography*, 2009, **65**, 148–155.

8 A. L. Spek, *Acta Crystallographica Section C Structural Chemistry*, 2015, **71**, 9–18.

9 S. Alvarez, P. Alemany, D. Casanova, J. Cirera, M. Llunell and D. Avnir, *Coordination Chemistry Reviews*, 2005, **249**, 1693–1708.

10 D. Gatteschi and L. Pardi, *Gazz. Chim. Ital.*, 1993, **123**, 231.

11 G. Gliemann, *Berichte der Bunsengesellschaft für physikalische Chemie*, 1985, **89**, 99–100.